Applying Different Vegetation Indices for Gross Primary Productivity Estimation in Soybean and Maize Based on a Modified Light-Use Efficiency Model

Zeyang Wei, Hai Xiao, Lu Zhang, Lifei Wei, and Qikai Lu

***Abstract*—Crop gross primary productivity (GPP) represents a fundamental variable for the investigation of carbon exchange dynamics among elements within agroecosystems. The usage of light use efficiency (LUE) models based on satellite data to estimate regional field GPP is regarded as an efficacious approach. The accuracy of conventional LUE models in estimating GPP is influenced by soil temperature dynamics and subsurface moisture conditions, both of which are challenging to fully characterize. Consequently, there is a necessity to enhance the LUE for soil temperature and soil moisture. Vegetation indices have been shown to effectively capture canopy dynamics and improve the accuracy of GPP estimation, with different indices yielding varying outcomes in LUE-based models. Therefore, in this study, we proposed a modified light use efficiency (M-LUE) model and quantified the influence of soil temperature on GPP estimation. The model was evaluated in three cropland sites, each characterized by distinct crop rotation systems and irrigation strategies. In addition, we tested the performances of nine vegetation indices in estimating the GPP. The results showed that M-LUE was accurate in GPP estimation with R_2 of 0.92±0.04 in maize and 0.81±0.05 in soybean. Compared to EC-LUE, M-LUE improved prediction accuracy in GPP estimation, especially for soybeans. For irrigated soybeans, the R_2 of M-LUE with EVI improved by 24.4%, while for rainfed soybeans, the R_2 of M-LUE with SR improved by 10.5%. In addition, the performance of the model is different between the irrigated and rainfed crops. It performed better in irrigated maize and rainfed soybean. The findings of this study demonstrate the considerable potential of the M-LUE model in the estimation of GPP for soybeans and maize.**

***Index Terms*—Eddy covariance, gross primary production, light use efficiency (LUE) model, M-LUE model, vegetation index.**

Received 28 November 2024; revised 5 April 2025; accepted 13 May 2025. Date of publication 29 May 2025; date of current version 13 June 2025. This work was supported in part by the National Natural Science Foundation under Grant 42271392, in part by the Opening Foundation of Xi'an Key Laboratory of Territorial Spatial Information under Grant 3001023545016, and in part by the Open Fund of Key Laboratory of Natural Resources Monitoring and Supervision in Southern Hilly Region, Ministry of Natural Resources under Grant NRMSSHR2022Y02 and Grant NRMSSHR2023Y03. *(Corresponding authors: Lifei Wei; Hai Xiao.)*

Zeyang Wei, Lu Zhang, Lifei Wei, and Qikai Lu are with the Faculty of Resources and Environmental Science, Hubei University, Wuhan 430062, China, and also with the Hubei Key Laboratory of Regional Development and Environmental Response, Hubei University, Wuhan 430062, China (e-mail: weizeyang0324@stu.hubu.edu.cn; 202021108011342@stu.hubu.edu.cn; weilifei2508@hubu.edu.cn; luqikai@hubu.edu.cn).

Hai Xiao is with the Second Surveying and Mapping Institute of Hunan Province, Changsha 410029, China, and also with the Key Laboratory of Natural Resources Monitoring and Supervision in Southern Hilly Region, Ministry of Natural Resources, Changsha 410029, China (e-mail: rshh2020@126.com).

Digital Object Identifier 10.1109/JSTARS.2025.3574163

I. Introduction

GROSS primary productivity (GPP) is the total amount of organic matter produced by plants through photosynthesis [1]. As the most significant contributor to the global ecosystem carbon exchange, GPP also has significant impacts on the food chain and sustainable human development. Currently, the cultivated cropland occupies about 24% of Earth's land surface [2], and crop GPP accounts for 15% of the global CO_2 fixation through photosynthesis [1]. Crop GPP is primarily influenced by the physical attributes of the cropland, species specificity of crops, and climatic conditions of the region. Each of these influencing factors itself results from the integrated effects of numerous fundamental components—such as soil properties, water availability, and management practices—that interact with one another [3], [4]. Among them, the soil water factors for GPP estimation might be the most important. Water content is reported to be a key factor affecting terrestrial crop GPP [5]. According to a study, compared to irrigated locations, net ecosystem exchange was significantly lower in rainfed sites during moisture stress times [6]. Furthermore, maize and soybean account for a significant proportion of global agricultural cropland, yet they exhibit disparate photosynthetic biochemical mechanisms. It is therefore necessary to obtain accurate GPP estimates for soybean and maize under prevailing irrigated and rainfed conditions, which will simultaneously facilitate an improvement in our understanding of crop growth and the carbon cycle.

At present, a large volume of eddy covariance system data has been distributed across global or regional flux networks, offering a viable avenue for precise and dependable estimation of GPP for an array of crop types. The eddy covariance tower measured CO_2 fluxes between the cropland surface and atmosphere with a high temporal resolution but over a limited area. For regional and global carbon exchange estimations, upscale beyond these tiny footprints is needed. Satellite remote sensing is an effective method for tracking crop yields, spatial patterns, and dynamic changes over time and space on a large regional scale [7], [8], [9].

At present, there are several methods for estimating GPP on a large scale: process-based models, sun-induced chlorophyll fluorescence (SIF) techniques [10], and light use efficiency (LUE) models. Each method presents unique advantages. Process-based models, such as the boreal ecosystem

productivity simulator and BIOME-BGC [11], simulate gross primary production by explicitly representing photosynthesis, respiration, and biogeochemical cycles. Although these models achieve high precision by resolving biophysical processes, their extensive reliance on parameterization and input data limits their scalability for regional or global applications. Similarly, the SIF–GPP relationship varies with vegetation type, canopy structure, and environmental factors, thus necessitating empirical or mechanistic adjustments to ensure robust and universal applicability.

GPP models using light use efficiency (LUE) theory and satellite reflectance data are often used to map spatial and temporal variations in GPP on a regional or global scale [12], [13], [14]. Many satellite-based LUE models have been developed in previous studies, including the MODIS-GPP model [15], VPM model [16], CI-LUE model [17], TEC model [18], EC-LUE model [19], CASA model [20], two-leaf LUE models [21], MVPM model [22], etc. Jiang et al. [23] demonstrated that the VPM model and EC-LUE performed better in simulating GPP. Yu [24] used the LUE-VPM model in conjunction with improved surface temperature data for the estimation of grass NPP. Biudes et al. [25] compared various GPP models using remote sensing data in southern Mato Grosso and observed significant seasonal variations in GPP between the wet and dry periods. Two-leaf LUE models, such as TL-LUE and RTL-LUE, partition the canopy into sunlit and shaded leaves, accounting for differing light absorption and saturation effects, thereby enhancing GPP estimation [26], [27].

The original LUE model still has some room for improvement. It is imperative that quantitative studies be conducted to ascertain the impact of environmental stress scalars and crop LUE as an accurate measure of crop yield, Bao et al. [30] identified temperature and soil water as the primary factors influencing LUE and soil moisture content as related to soil temperature. A recent study coupled the LUE_{max} with new temperature stress and obtained better performance than the MODIS model, especially for croplands of evergreen broadleaf forests [31]. Yang et al. [32] indicated that the fraction of diffuse radiation played a crucial role as the main factor influencing the LUE of winter wheat. It could account for as much as 55% of the variability in LUE across eight eddy covariance sites within the field ecosystems located in the North China Plain. Spatial differences in elements such as solar radiation, air temperature, soil temperature, and humidity give rise to differing physiological stresses on photosynthesis across plant species [33], [34], [35]. Furthermore, GPP is more closely linked to the primary temperature regulation of air or soil. Thus, satellite-based GPP models should consider climate stress to photosynthesis in GPP estimation. In addition, fraction of photosynthetically Active Radiation (fPAR) is another significant parameter in the LUE model [28], [29]. Several studies have indicated that fPAR is associated with the vegetation index across various biomes [36], [37], [38], [39], [40]. The impact of vegetation indices on fPAR in the GPP estimation model is important. It is worth exploring the effect of different vegetation indices on LUE modeling.

In this study, we enhance the LUE model by incorporating a range of temperature-related factors. A modified LUE (M-LUE) model is proposed, in which the performances of M-LUE for irrigated and rainfed crops are compared for GPP estimation. The objectives of this research are as follows.

1) To propose a M-LUE model to estimate GPP.
2) To test the performances of M-LUE for soybeans and maize GPP estimation under different crop growth environments.
3) To evaluate the performance of several of the more widely used vegetation species in the M-LUE model.

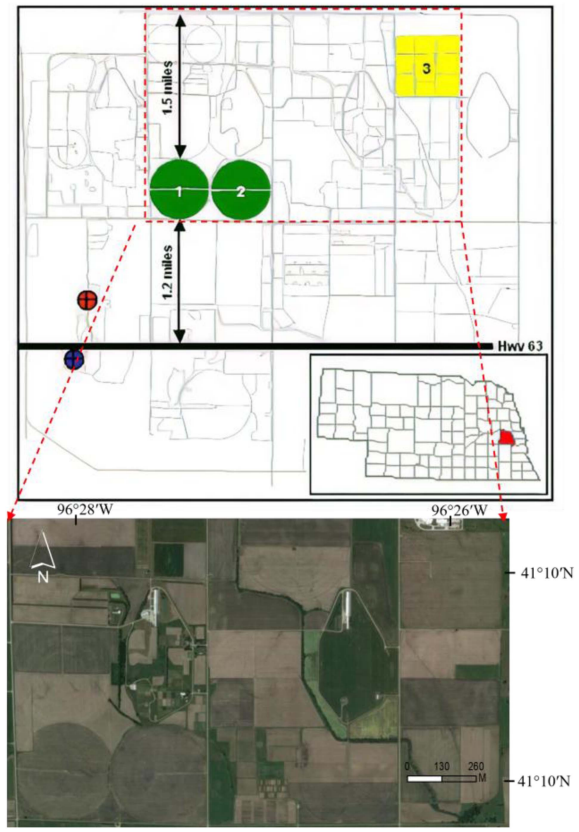

Fig. 1. Geographical location of three study sites in Mead, Nebraska, America.

II. Study Area and Materials

A. Study Area

In this study, we tested three cropland sites during the growing seasons from 2003 to 2012. The study sites are situated within 1.6 km of each other at the University of Nebraska Agricultural Research and Development Center in Mead, Nebraska, USA, as shown in Fig. 1. Sites 1 and 2 are irrigated and supplied with water using artificial devices, while Site 3 receives water only from rainfall. Before the study began, Sites 1 and 2 had been farmed with soybeans and corn on a rotational basis for the past 10 years, while Site 3 has been planted with a variety of crops, including wheat, soybeans, oats, and maize. The three sites have followed no-till management since 2001. Site 1 has always been planted to corn, while Sites 2 and 3 are planted to maize in odd-numbered years and soybeans in the rest of the year.

B. Dataset

The flux tower eddy covariance data were collected from the FLUXNET2015'.[1] The data used include air temperature, sensible heat flux, latent heat flux, soil heat flux, shortwave radiation, net radiation, and GPP during the growing seasons from 2003 to 2012, with a daily temporal resolution. CO_2 fluxes, water vapor, and energy fluxes were measured by the equipped eddy covariance tower and meteorological sensors, explaining approximately 90%–95% of the flux footprint during daytime and 70%–90% during nighttime, respectively [41]. To guarantee sufficient upwind fetch from every direction and gather hourly data on CO2 fluxes, the following installation procedures were carried out for eddy covariance sensors. When the height of the canopy is less than 1 m, the sensors are initially positioned at an elevation of 3 m above the ground, and subsequently elevated to a height of 6.2 m, which remains in place until the commencement of the harvest season [6]. In this study, the "GPP_DT_VUT_REF" variable (GPP, gC/m²/d) was used to estimate GPP, which was derived from daytime NEE using a hyperbolic light response curve. This method was adjusted to account for the effects of temperature and vapor pressure deficit (VPD) on photosynthesis. Meanwhile, the model efficiency method was used to filter different friction velocity thresholds in the NEE data. Ecosystem respiration (Re) was estimated based on the ordinate intercept. (Details are given on the website description on 'FLUXNET2015 Datasets').

For vegetation indices, we used the 16-day MODIS Vegetation Indices product (MOD13Q1) with a spatial resolution of 250 m and the 8-day MODIS Surface Reflectance product (MOD09A1) at a 500 m resolution. The pixel selection criterion is based on the secondary product results with the best data quality during the revisit period, along with providing quality correction data. Vegetation index spikes caused by rain, snow, or clouds were smoothed using a double logistic method [23]. Gaps in spectral reflectance and meteorological data are filled by bilinear interpolation based on available long-time-series observations [23].

III. Methods

A. M-LUE Model

The LUE model is predicated on the assumption that ecosystem GPP is directly proportional to PAR and LUE. It is possible that LUE predictions may be lower than actual values as a result of changes in external environmental conditions, such as low temperatures.

Water stress using VPD is widely used in LUE-GPP models to measure the effect of temperature on GPP. However, it is difficult to measure high-precision soil moisture data on a regional scale [42]. And there is not a simple linear relationship between VPD and soil moisture [19]. Quantifying the effect of soil temperature on photosynthesis in isolation is a challenge because GPP is closely related to air temperature as well as soil temperature.

[1][Online]. Available at: http://fluxnet.fluxdata.org/data/fluxnet2015-dataset/.

To address these limitations, we explored an approach that leverages the soil surface heat budget to better represent the impact of soil temperature on photosynthesis. This modification provides a more physically based assessment by integrating latent heat, soil heat flux, and sensible heat flux, which together capture the combined influence of soil moisture and temperature on crop productivity.

The heat budget of the ground can be expressed by the ground heat balance equation

$$\mathrm{Rn} = \mathrm{LE} + G + H \tag{1}$$

where Rn, LE, G, and H are net radiation (MJ/m^2/d), latent heat (MJ/m^2/d), soil heat flux (MJ/m^2/d), and sensible heat flux (MJ/m^2/d). These factors were combined to create the new temperature stress T_{s2}, which is a combined representation of soil temperature and moisture conditions. LUEmax represents the maximum LUE under optimal conditions, without environmental stress, and is associated with different vegetation community types. In this study, LUEmax was set to 2.94 for maize and 1.45 for soybean, as defined by Jiang et al. [23]

$$\mathrm{GPP} = \mathrm{PAR} \times fPAR \times LUE_{\max} \times f \tag{2}$$

$$f = \mathrm{Min}\left(T_{s1}, T_{s2}\right) \tag{3}$$

$$T_{s1} = \begin{cases} \frac{(T_a - T_{\min}) \times (T_a - T_{\max})}{\left((T_a - T_{\min}) \times (T_a - T_{\max}) - (T_a - T_{\mathrm{opt}})^2\right)} & T_{\min} < T_a < T_{\max} \\ 0 & T_a < T_{\min} \text{ or } T_a > T_{\max} \end{cases} \tag{4}$$

$$T_{s2} \begin{cases} 0 & T_a < T_{\min} \\ \frac{T_a \times \mathrm{LE} \times (R_n - G}{T_{\mathrm{opt}} \times R_n \times (\mathrm{LE} + H)} & T_{\min} \le T_a \le T_{\mathrm{opt}} \\ \frac{\mathrm{LE} \times (R_n - G)}{R_n \times (\mathrm{LE} + H)} & T_a > T_{\mathrm{opt}} \end{cases} \tag{5}$$

where $T_{\min}$, $T_{\max}$, and T_{opt} refer to the daily minimum, maximum, and optimal air temperatures (°C) for crop photosynthesis, respectively. In this study, $T_{\min}$, $T_{\max}$, and T_{opt} were set to 0, 45, 27.38 °C for maize and -3, 42, 24.83 °C for soybean [43]. In addition, the meteorological data including LE, Rn, G, H, and air temperature (°C) were collected by meteorological sensors. These factors can be derived from land surface temperature products.

B. fPAR Estimation

As a leaf pigment, chlorophyll is of vital significance for absorbing and intercepting radiation through photosynthesis. Total canopy chlorophyll content is a key factor influencing vegetation productivity. In addition, vegetation indices are closely linked to chlorophyll content, and in crops, the total canopy chlorophyll is a major driver of GPP [44]. Currently, in the calculation of crop GPP, the vegetation index is generally applied to calculate fPAR. In this study, various commonly used vegetation indices were evaluated for fPAR estimation, as shown in Table I, with spectral reflectance data sourced from MOD09A1 (Green: 545–565 nm, Red: 620–670 nm, NIR: 841–876 nm) and MOD13Q1 (NDVI: band1, EVI: band2). Since fPAR is linearly correlated with

TABLE I
DESCRIPTION OF THE NINE VEGETATION INDICES USED IN THIS STUDY

Vegetation Indices	Formula	Reference
NDVI	$(\rho_{NIR}-\rho_{Red})/(\rho_{NIR}+\rho_{Red})$	Rouse et al. (1973)
EVI	$2.5\times(\rho_{NIR}-\rho_{Red})/(1+\rho_{NIR}+6.0\times\rho_{Red}-7.5\times\rho_{Blue})$	Huete (1995)
EVI2	$2.5\times(\rho_{NIR}-\rho_{Red})/(1+\rho_{NIR}+2.4\times\rho_{Red})$	Jiang et al. (2008)
RDVI	$\rho_{NIR}\rho_{Red}/\sqrt{\rho_{NIR}+\rho_{Red}}$	Roujean et al. (1995)
SR	ρ_{NIR}/ρ_{Red}	Jordan (1969)
CI_{green}	$\rho_{NIR}/\rho_{Green}-1$	Gitelson et al. (2003)
SAVI	$(\rho_{NIR}-\rho_{Red})(1+L)/(\rho_{NIR}+\rho_{Red}+L)$	Huete (1988)
MSAVI	$\rho_{NIR}+0.5-0.5\sqrt{(2\rho_{NIR}+1)^2-8(\rho_{NIR}-\rho_{Red})}$	Qi et al. (1994)
OSAVI	$(\rho_{NIR}-\rho_{Red})/(\rho_{NIR}+\rho_{Red}+0.16)$	Rondeaux et al. (1996)

* In the original formulation (Huete, 1988), L is a scalar varying from 0 to 1. For low to moderate vegetation density, L was set to 0.5 based on previous studies, so we calculated SAVI as $(\rho_{NIR}-\rho_{Red})\times1.5/(\rho_{NIR}+\rho_{Red}+0.5)$ for soybean and maize.

vegetation indices, the fPAR model can be expressed as

$$\mathrm{fPAR} = m\times\mathrm{VI}-n \tag{6}$$

where m and n are empirical constants. In this formulation, the constant m represents the scaling factor that quantifies the sensitivity of fPAR to changes in the vegetation index, while n accounts for any offset due to background effects or intrinsic sensor characteristics. This linear model is based on the assumption that the chlorophyll-related absorption properties of the canopy are directly reflected in the measured VI values, making it a practical and robust approach for GPP estimation under the conditions evaluated in our study.

C. Evaluation Metrics

Four metrics were used to assess model performance: coefficient of determination (R^2), mean absolute error (MAE), root mean squared error (RMSE), and mean predictive error (BIAS). Simulated GPP was compared with ground-based GPP from EC flux towers. Better GPP estimation is indicated by higher R^2 and lower RMSE, MAE, and BIAS. These indicators are expressed as follows [45], [46], [47]:

$$R^2 = \frac{\sum_{i=1}^{n}\left(O_i-\bar{O}\right)\left(P_i-\bar{P}\right)}{\sqrt{\sum_{i=1}^{n}\left(O_i-\bar{O}\right)^2\cdot\left(P_i-\bar{P}\right)^2}} \tag{7}$$

$$\mathrm{MAE} = \frac{\sum|O_i-P_i|}{N} \tag{8}$$

$$\mathrm{RMSE} = \sqrt{\frac{\sum\left(O_i-P_i\right)^2}{N}} \tag{9}$$

$$\mathrm{BIAS} = \frac{\sum\left(P_i-O_i\right)}{N} \tag{10}$$

where O_i is the estimated value and P_i is the GPP value called "GPP_DT_VUT_REF" from the 'FLUXNET2015 Datasets', $\bar{O}$, $\bar{P}$represents the average of the estimated values and simulated values, respectively. N represents the total number of observations.

IV. RESULTS

A. M-LUE Performance Under Different Vegetation Indices

Coefficients m and n (listed in Table II) are critical for accurate GPP estimation. As indicated in (2), these calibrated parameters differ significantly between soybean and maize, primarily due to the inherent biochemical differences between the crops. Moreover, the choice of vegetation index can influence the fPAR estimation [48]; for instance, NDVI is more affected by soil background effects when fPAR is below 0.5, whereas SAVI is more effective in minimizing such influences [38]. Previous studies have also shown that indices such as SAVI, RDVI, and EVI can alleviate issues related to vegetation background interference, saturation phenomena, and atmospheric disturbances [49], [50]. In addition, EVI is particularly sensitive to slight increases in canopy density as the crop canopy develops.

Fig. 2 demonstrates the performance of GPP estimation for soybean and maize using various vegetation indices within the M-LUE framework. Four performance metrics—R^2, MAE, RMSE, and BIAS—were calculated for both irrigated and rainfed sites. All tested indices provided reliable GPP estimates, with BIAS below 0.54 gC/m²/d, R^2 values ranging from 0.92 ± 0.04 in maize to 0.81 ± 0.05 in soybean. Among these, OSAVI exhibited the best overall performance for both crops.

Notably, the vegetation indices performed better for maize than for soybeans. On average, maize GPP estimates achieved $R^2 = 0.94$, MAE = 1.85 gC/m²/d, and RMSE = 2.32 gC/m²/d,

TABLE II
MODEL PARAMETERS OF FPAR ESTIMATION FOR SOYBEAN AND MAIZE IN THE M-LUE MODEL UNDER DIFFERENT CULTIVATED CONDITIONS

VI	Best fit function			
	Maize		Soybean	
	Irrigated	Rainfed	Irrigated	Rainfed
NDVI	fPAR = 0.95x-0.182	fPAR = 0.95x-0.164	fPAR = 0.70x+0.295	fPAR = 0.98x-0.004
EVI	fPAR = 1.09x-0.083	fPAR = 1.03x-0.021	fPAR = 1.31x+0.067	fPAR = 1.31x-0.054
EVI2	fPAR = 1.09x-0.044	fPAR = 1.25x-0.075	fPAR = 1.64x-0.082	fPAR = 1.31x+0.071
RDVI	fPAR = 1.23x-0.060	fPAR = 1.71x-0.237	fPAR = 1.64x-0.002	fPAR = 2x-0.179
SR	fPAR = 0.17x+0.373	fPAR = 0.82x-0.052	fPAR = 0.35x+0.511	fPAR = 0.34x+0.451
CI_{green}	fPAR = 1.05x-0.035	fPAR = 1.25x-0.044	fPAR = 1.34x+0.080	fPAR = 1.34x+0.085
SAVI	fPAR = 1.23x-0.091	fPAR = 1.31x-0.091	fPAR = 1.64x-0.048	fPAR = 1.64x-0.063
MSAVI	fPAR = 1.23x-0.111	fPAR = 1.31x-0.092	fPAR = 1.64x-0.074	fPAR = 1.64x-0.072
OSAVI	fPAR = 1.23x-0.120	fPAR = 1.31x-0.130	fPAR = 1.64x-0.081	fPAR = 1.64x-0.095

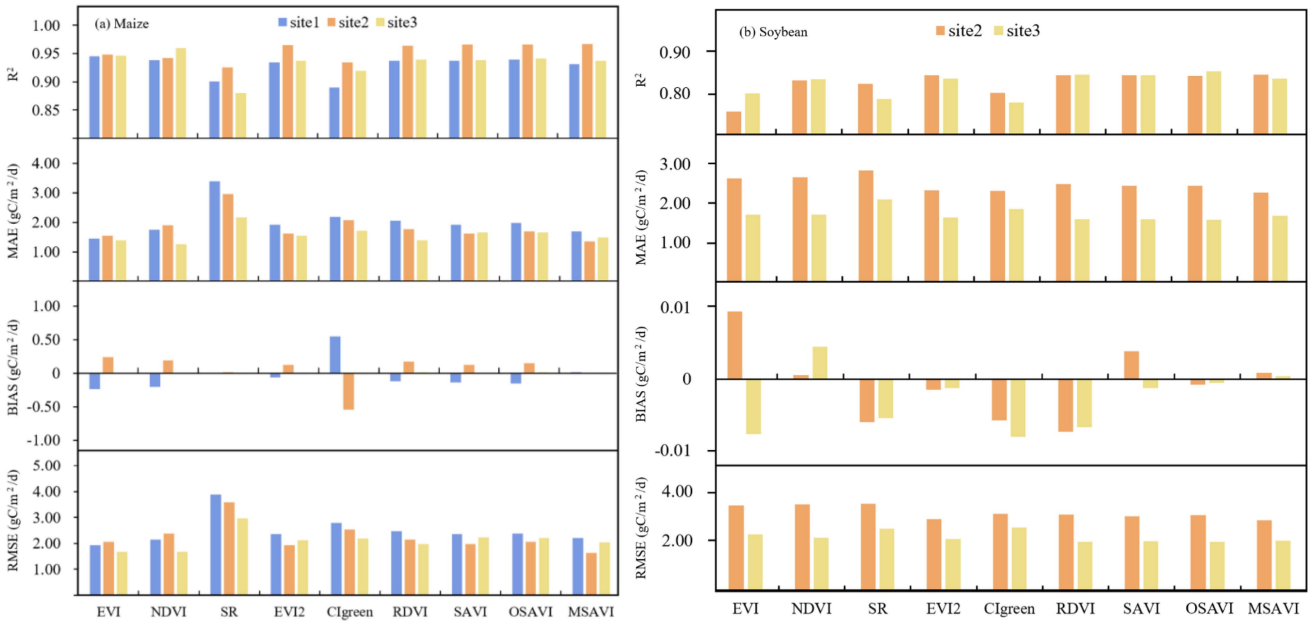

Fig. 2. Model performances with nine vegetation indices in (a) maize and (b) soybean for simulating growing season daily GPP under different cultivated conditions.

compared to soybean estimates with R^2 = 0.83, MAE = 2.12 gC/m²/d, and RMSE = 2.65 gC/m²/d.

Furthermore, model performance varied with crop management practices. In the study, twenty croplands were evaluated—ten under irrigated management and ten relying on rainfall. All sites obtained higher yields and nitrogen efficiency than conventional cropland, and site1 and site2 had higher crop densities than site3 [51]. For maize, all vegetation indices yielded superior performance in irrigated fields compared to rainfed ones. Conversely, for soybeans, the indices performed better in rainfed conditions. For example, MSAVI attained the highest R^2 (0.97) for irrigated maize, whereas OSAVI reached the highest R^2 (0.76) for rainfed soybeans. In irrigated crops, MSAVI, SAVI, and EVI2 generally provided higher R^2 values, while for rainfed crops, EVI, OSAVI, and RDVI were more effective.

The performance comparison was further extended to different cropping systems. In the case of maize, the indices were evaluated for continuous (Site 1) versus rotation (Site 2) cropping. All vegetation indices performed better in rotation fields, with average metrics of $R^2 = 0.95$, MAE = 1.86 gC/m²/d, and RMSE = 2.27 gC/m²/d, compared to $R^2 = 0.93$, MAE = 2.09 gC/m²/d, and RMSE = 2.56 gC/m²/d in continuous fields. Notably, EVI, NDVI, and RDVI were particularly effective in estimating GPP in continuous cropland, while OSAVI maintained high performance across both cropping systems (R^2 ranging from 0.94 to 0.97). Overall, the results indicate that the M-LUE model successfully captures the temporal dynamics of GPP in agroecosystems, with indices such as MSAVI and SAVI achieving precise GPP estimates in rotation croplands (RMSE below 2.46 gC/m²/d and R^2 values exceeding 0.97).

B. Comparison With the Other LUE Models

A comparison was conducted between the results obtained from the M-LUE model and those derived from five other commonly used models, namely EC-LUE, VPM, MODIS-GPP, CI-LUE, and MVPM, at the selected testing sites. The model outputs were aggregated over 16-day intervals to align with the time scale of MODIS products. The M-LUE model outperforms the other five models at these sites, based on R^2, MAE, RMSE, and BIAS values (see Table III). Notably, the M-LUE model improved prediction accuracy in GPP estimation for soybean and maize. And the improvement was more obvious in soybeans. The M-LUE model performed better than the other models for soybean and maize due to the consideration of the soil temperature factor and latent heat flux. The M-LUE model explained 91% of the variation in the 16-day GPP, whereas MODIS-GPP, EC-LUE, VPM, M-VPM, and CI-LUE explained 85%, 86%, 85%, 82%, and 85%, respectively. From the MAE results, M-LUE is lower than other LUE models at several sites. As to the BIAS values, the results from M-LUE were closer to zero, but the average bias value for the other models was 0.43. In addition, M-LUE obtained the lowest RMSE average value of 2.3. Overall, the M-LUE model obtained better predictions in GPP estimation than the other tested LUE models.

V. Discussion

A. Seasonal Dynamics of GPP and NEE

Fig. 3 shows the seasonal patterns of observed NEE and GPP at three eddy covariance flux tower sites for soybean and maize. Daytime actual GPP was calculated by subtracting NEE from Re [52].

Soybeans and maize differ in the specific biochemical mechanisms involved in photosynthesis. The maize growing season lasted from early May to late September. And maize was planted when average temperatures above 10 °C. Seeds germinate between 5 and 30 days after sowing. By mid-June, significant changes in NEE (>1 gC/m^2/d) had been observed. Then, both values of GPP and NEE increased rapidly and peaked in early July. Once the previous quarter's peak is reached, the GPP and NEE quickly decrease to 0 again in early October, after which farmers left the crop in the fields to dry for a few days before harvesting. The harvest time of maize was in mid to late October at the tested sites.

As for soybeans, the crop-growth seasons were from mid-late May to late October. Studies showed that soybean seed geminates and emerges in 8–10 days [53]. By late June, significant changes in NEE (>1 gC/m^2/d) had been detected. GPP and NEE both increased sharply, reaching a peak in early August. Afterward, they gradually declined and neared zero by late September, indicating that the soybean was ready for harvest. Both GPP and NEE remained around zero after harvest [see Fig. 3(d) and (e)].

In addition, the growing season precipitation accounts for about 55% of the annual precipitation. And the moisture captured by Site 1 and Site 2 were twice as much as that of Site 3. As crops in Site 3 rely entirely on rainfall for moisture and sowed approximately 30% fewer crop seeds per acre than the irrigated sites, the flux in Site 3 was lower than that in Site 1 or Site 2 (see Fig. 3).

B. Comparison of Model Performance in Soybean and Maize

Linear regressions between actual GPP and VI×PAR×$\mathrm{LUE}_{\max}\times f$ during the growing season for each site were calculated. Figs. 4–6 presented the results of maize in Site 1, Site 2, and Site 3, respectively. Fig. 7 and 8 showed the results of soybean in Site 2 and Site 3, respectively. The performance of M-LUE with vegetation indices was different for soybean and maize.

The model with OSAVI performed best than the model with other vegetation indices. It accounted for 94% (maize in Site 1 and Site 3), 97% (maize in Site 2), 84% (soybean in Site 2), and 86% (soybean in Site 3) of GPP variations. The results showed that the model with RDVI, OSAVI, and SAVI performed better for irrigated maize sites. And the model with NDVI and EVI, presented better results for rainfed maize sites. Furthermore, for soybeans, the model with EVI2 and MSAVI performed better in irrigated fields, while the model with RDVI worked best in rainfed crops.

In addition, chloroplasts on the leaf surface primarily absorb visible light, and research has shown that C3 plants typically have higher chlorophyll content than C4 plants [44]. Total chlorophyll in the plant canopy is equal to the product of canopy leaf area and leaf chlorophyll content. Thus, it can be found that the reflectance of soybean is lower than that of maize in the visible wavelengths at the same total chlorophyll content. In addition, leaf scattering has the greatest impact on NIR reflectance, soybean leaf reflectance was higher than maize leaf in this band [54]. As a result, soybeans have a lower visible reflectance and a higher NIR reflectance than maize, and causes the vegetation indices using reflectance in these two bands to vary between soybeans and maize.

C. Model Uncertainty

Model uncertainties are inherited from several factors including the eddy covariance data, the model structure, and the satellite-based vegetation indices. In this study, M-LUE was

TABLE III
MODEL PERFORMANCE OF SIX LUE MODELS

Site	Model	R^2	MAE	RMSE	BIAS
Site1-Maize N=87	M-LUE	0.9394	1.9848	2.3797	-0.1513
	MODIS-GPP	0.9259	2.2457	2.8798	1.2845
	EC-LUE	0.9401	3.1450	3.8820	-2.8896
	VPM	0.8854	2.2536	2.9147	-0.4225
	M-VPM	0.8738	2.3512	3.1112	0.9230
	CI-LUE	0.9259	5.6159	6.9935	5.4024
Site2-Maize N=46	M-LUE	0.9654	1.6968	2.0554	0.1432
	MODIS-GPP	0.9409	2.3897	2.9668	1.2931
	EC-LUE	0.9470	2.6529	3.3439	-2.3439
	VPM	0.9390	1.7178	2.1989	-0.0567
	M-VPM	0.9119	2.2499	2.8563	0.6787
	CI-LUE	0.9409	5.7155	7.3254	5.5279
Site3-Maize N=41	M-LUE	0.9409	1.6453	2.2173	0.0095
	MODIS-GPP	0.9074	2.7108	3.3294	-0.0073
	EC-LUE	0.9532	1.6672	2.1663	-1.1749
	VPM	0.9226	1.6580	2.1663	-0.0035
	M-VPM	0.8892	2.8991	3.6495	-0.0163
	CI-LUE	0.9074	5.6662	7.1621	0.0096
Site2-Soybean N=38	M-LUE	0.8434	2.4513	3.0491	-0.0008
	MODIS-GPP	0.6230	4.4827	6.1707	-0.0250
	EC-LUE	0.6779	3.3803	4.5055	2.1013
Site	Model	R^2	MAE	RMSE	BIAS
Site3-Soybean N=36	VPM	0.7041	3.5333	4.7847	-0.0216
	M-VPM	0.5642	3.9986	5.8405	-0.0185
	CI-LUE	0.6230	5.3321	7.1230	-0.0166
	M-LUE	0.8554	1.5904	1.9550	-0.0005
	MODIS-GPP	0.8495	3.1617	3.6893	-0.0055
	EC-LUE	0.7741	1.9114	2.4413	0.5377
	VPM	0.8086	2.0565	2.5032	-0.0051
	M-VPM	0.8412	2.9529	3.4079	-0.0016
	CI-LUE	0.8495	4.2370	4.8914	0.0576

relied on the eddy covariance data and studies have found that the flux data may cause some uncertainties in GPP estimation [55]. For example, using the gap filling methods may cause 10%–30% errors to flux data [56]. Recent studies further highlight that the reconstruction of key change points in temporally continuous gaps (e.g., cloud contamination) can lead to divergent performance in GPP estimation across latitudes and seasons, especially in equatorial regions with complex phenology [57]. In addition, the partition method of NEE to GPP and Re also causes uncertainties due to the lack consideration of ecosystem processes and environmental conditions [58]. Therefore, there is a need to improve the methodology for estimating GPP and Re

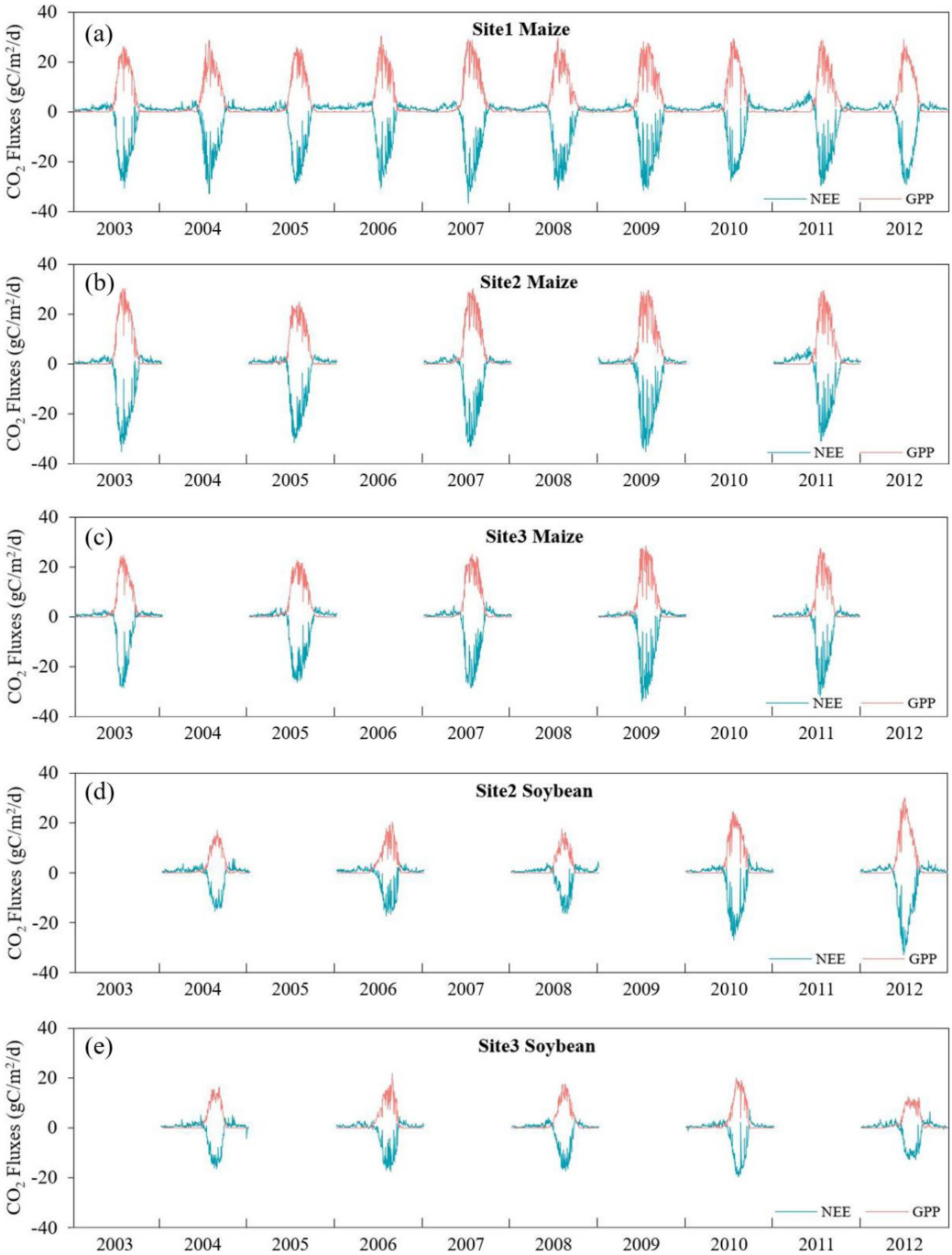

Fig. 3. Seasonal dynamics and interannual variation of NEE and GPP observed by eddy covariance flux tower sites in Mead, Nebraska, during 2003–2012. (a) Irrigated, continuously maize site. (b) Irrigated, rotation maize site. (c) Rainfed, rotation maize site. (d) Irrigated, rotation soybean site. (e) Rainfed, rotation soybean site.

using NEE in the follow-up work. Besides, the model structure may cause some uncertainties, such as the selection of environmental stress. The environmental stress function can be expressed in an additive form, a minimal form or more complex mathematical form [59], [60], [61]. Moreover, the choice of vegetation indices (e.g., MODIS FAPAR versus Sentinel-3 OLCI FAPAR) introduces variability, as their data quality (e.g., temporal resolution, noise filtering) significantly impacts GPP accuracy [62]. For instance, fPAR values derived from vegetation indices are often overestimated due to saturation effects in dense canopies [46]. Notably, while advanced filtering methods (e.g., SeasonL1) have improved GPP simulations (R^2 increments up to 0.07), their efficacy remains context-dependent, with uncertainties persisting in regions with rapid phenological shifts [57]. Apart from these factors, model uncertainties may come from MODIS sensor viewing angles [63], model parameter calibration [64], *N* deposition, CO2 fertilization, and field management.

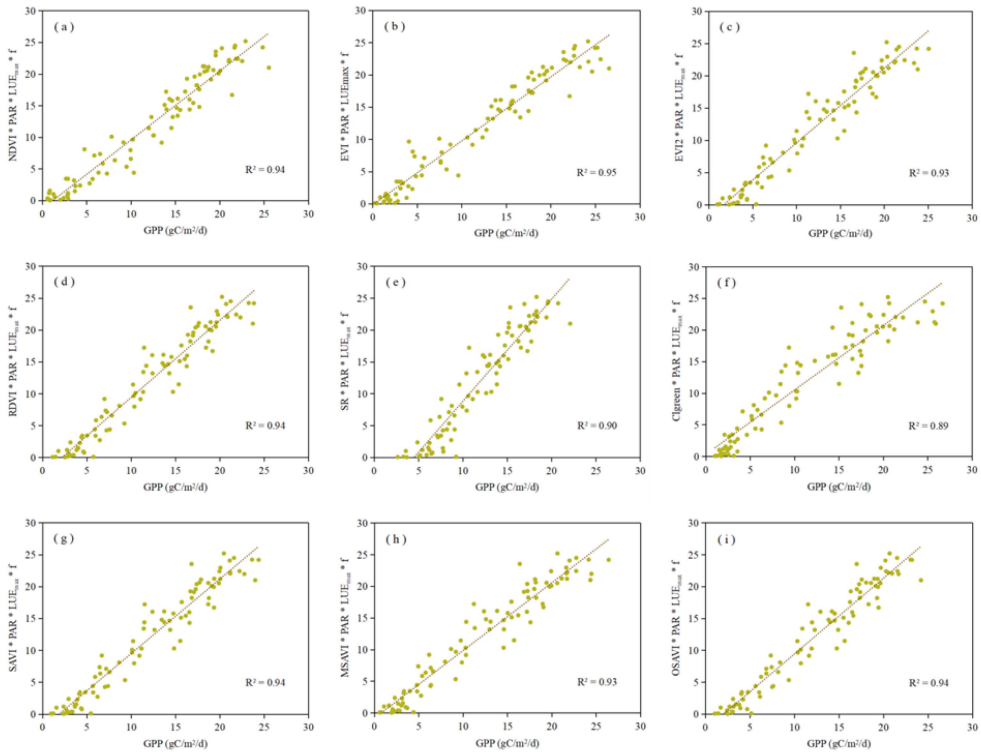

Fig. 4. Relationship between actual GPP and predicted GPP for maize data collected at Site 1 in 2003, 2005, 2007, 2009, and 2011. Panels (a)–(i) correspond to the vegetation indices used in the GPP prediction: (a) NDVI, (b) EVI, (c) EVI2, (d) RDVI, (e) SR, (f) CIgreen, (g) SAVI, (h) MSAVI, and (i) OSAVI.

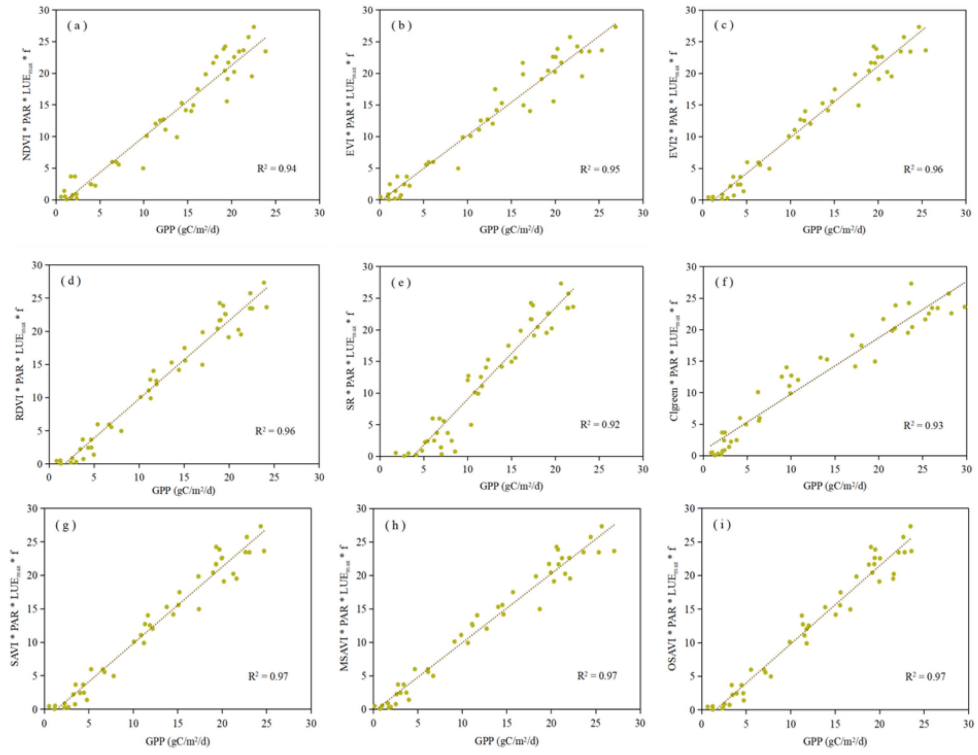

Fig. 5. Relationship between actual GPP and predicted GPP for maize data collected at Site 2 in 2003, 2005, 2007, 2009, and 2011. Panels (a)–(i) correspond to the vegetation indices used in the GPP prediction: (a) NDVI, (b) EVI, (c) EVI2, (d) RDVI, (e) SR, (f) CIgreen, (g) SAVI, (h) MSAVI, and (i) OSAVI.

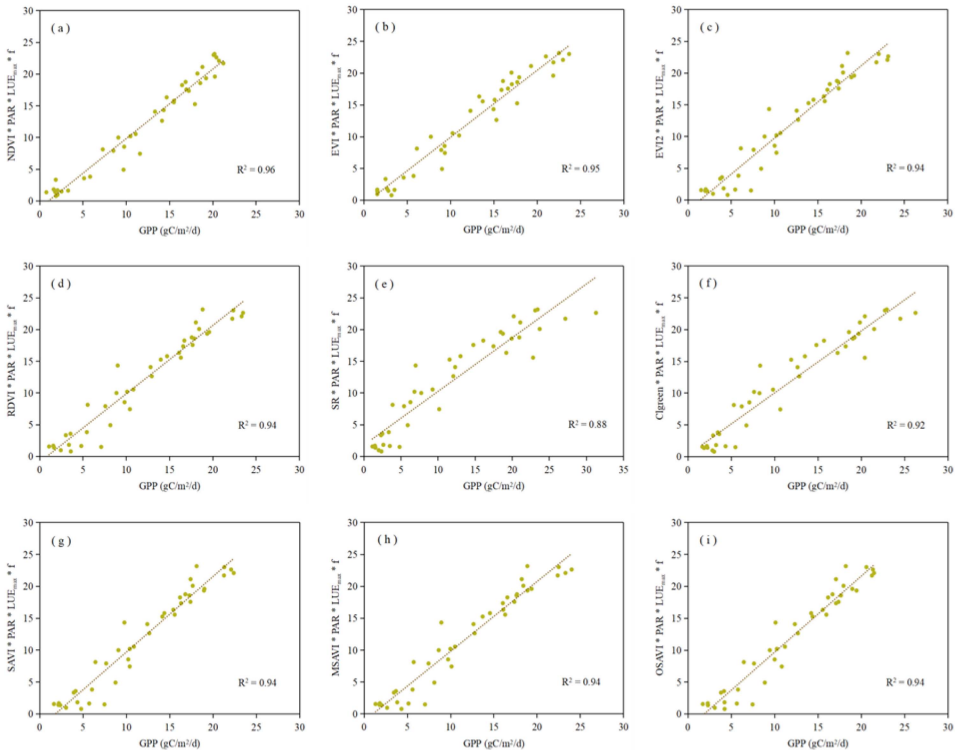

Fig. 6. Relationship between actual GPP and predicted GPP for maize data collected at Site 3 in 2003, 2005, 2007, 2009, and 2011. Panels (a)–(i) correspond to the vegetation indices used in the GPP prediction: (a) NDVI, (b) EVI, (c) EVI2, (d) RDVI, (e) SR, (f) CIgreen, (g) SAVI, (h) MSAVI, and (i) OSAVI.

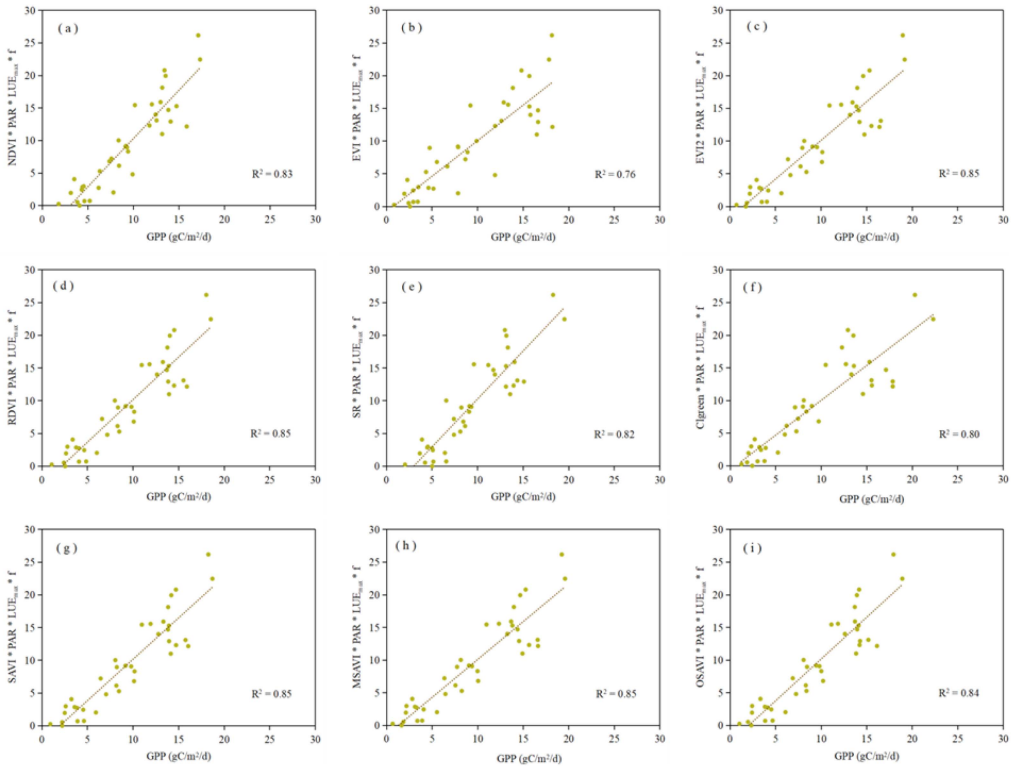

Fig. 7. Relationship between actual GPP and predicted GPP for soybean data collected at Site 2 in 2004, 2006, 2008, 2010, and 2012. Panels (a)–(i) correspond to the vegetation indices used in the GPP prediction: (a) NDVI, (b) EVI, (c) EVI2, (d) RDVI, (e) SR, (f) CIgreen, (g) SAVI, (h) MSAVI, and (i) OSAVI.

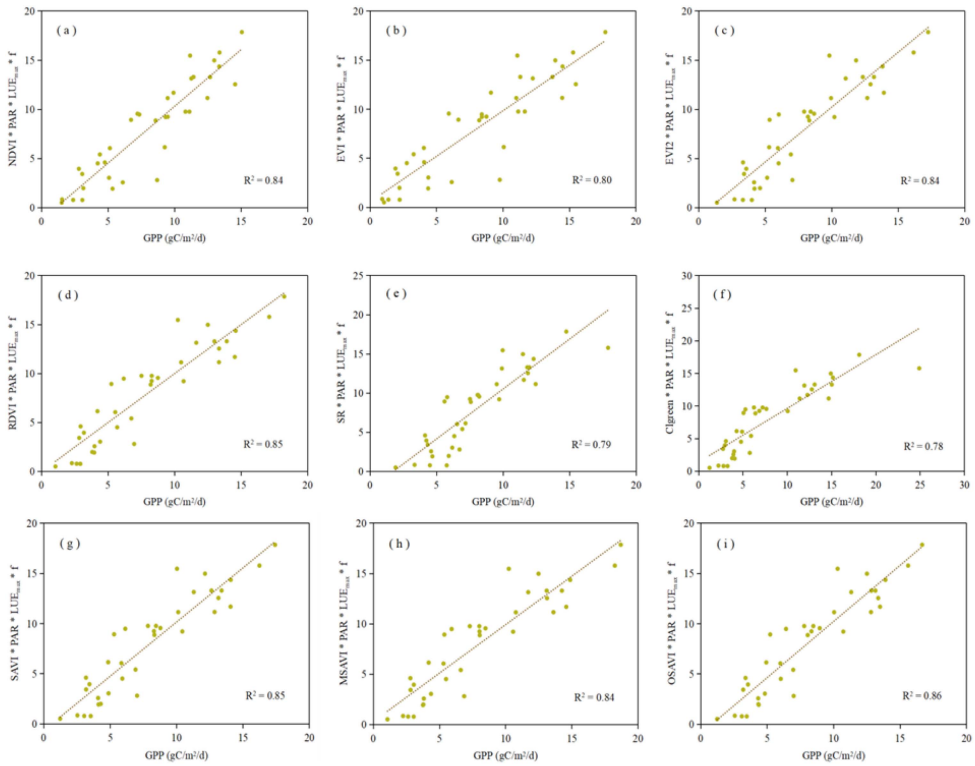

Fig. 8. Relationship between actual GPP and predicted GPP for soybean data collected at Site 3 in 2004, 2006, 2008, 2010, and 2012. Panels (a)–(i) correspond to the vegetation indices used in the GPP prediction: (a) NDVI, (b) EVI, (c) EVI2, (d) RDVI, (e) SR, (f) CIgreen, (g) SAVI, (h) MSAVI, and (i) OSAVI.

VI. Conclusion

This study aimed to enhance the LUE model and conduct a comprehensive evaluation of the M-LUE model using different vegetation indices for soybean and maize. We utilized data from three sites under both irrigated and rainfed conditions over a 10-year period (2003–2012).

The comparison with other LUE models revealed that the M-LUE model achieved higher R^2 values and provided better GPP predictions. The results demonstrated that the M-LUE model accurately estimated GPP for both soybean and maize.

Among different vegetation indices, the model using OSAVI, SAVI, and RDVI performed best in predicting GPP for these crops. In addition, the M-LUE model showed varying performance under artificial irrigation and natural rainfed conditions. Specifically, its performance was better for maize under artificial irrigation and for soybeans under rainfed conditions.

The M-LUE model holds great potential for precision irrigation estimation, crop production management, and field rotation strategies. It also provides a framework for large-scale GPP estimation. Future improvements should focus on reducing GPP estimation errors to enhance the model's accuracy and reliability.

References

[1] C. M. Malmström, M. V. Thompson, G. P. Juday, S. O. Los, J. T. Randerson, and C. B. Field, "Interannual variation in global-scale net primary production: Testing model estimates," *Glob. Biogeochemical Cycles*, vol. 11, pp. 367–392, 1997, doi: 10.1029/97GB01419.

[2] K. Cassman and S. Wood, "Cultivated systems," *Ecosystems Hum. Well-Being, Curr. State Trends*, vol. 1, pp. 745–794, 2005.

[3] J. Ping and A. Dobermann, "Processing of yield map data," *Precis. Agriculture*, vol. 6, pp. 193–212, 2005, doi: 10.1007/s11119-005-1035-2.

[4] J. Ping, R. Ferguson, and A. Dobermann, "Site-specific nitrogen and plant density management in irrigated maize," *Agronomy J.*, vol. 100, pp. 1193–1204, 2008, doi: 10.2134/agronj2007.0174.

[5] Z. Sun et al., "Evaluating and comparing remote sensing terrestrial GPP models for their response to climate variability and CO2 trends," *Sci. Total Environ.*, vol. 668, pp. 696–713, 2019, doi: 10.1016/j.scitotenv.2019.03.025.

[6] A. E. Suyker, S. B. Verma, G. G. Burba, T. J. Arkebauer, D. T. Walters, and K. G. Hubbard, "Growing season carbon dioxide exchange in irrigated and rainfed maize," *Agricultural Meteorol.*, vol. 124, pp. 1–13, 2004, doi: 10.1016/j.agrformet.2004.01.011.

[7] Y. Peng and A. A. Gitelson, "Application of chlorophyll-related vegetation indices for remote estimation of maize productivity," *Agricultural Meteorol.*, vol. 151, pp. 1267–1276, 2011, doi: 10.1016/j.agrformet.2011.05.005.

[8] Y. Peng, A. A. Gitelson, and T. Sakamoto, "Remote estimation of gross primary productivity in crops using MODIS 250m data," *Remote Sens. Environ.*, vol. 128, pp. 186–196, 2013, doi: 10.1016/j.rse.2012.10.005.

[9] H. Wu et al., "A review of crowdsourced geographic information for land-use and land-cover mapping: Current progress and challenges," *Int. J. Geographical Inf. Sci.*, vol. 38, no. 11, pp. 2183–2215, Nov. 2024, doi: 10.1080/13658816.2024.2379468.

[10] C. Y. Chang et al., "Unpacking the drivers of diurnal dynamics of sun-induced chlorophyll fluorescence (SIF): Canopy structure, plant physiology, instrument configuration and retrieval methods," *Remote Sens. Environ.*, vol. 265, Nov. 2021, Art. no. 112672, doi: 10.1016/j.rse.2021.112672.

[11] S. Qiu et al., "Estimation of European terrestrial ecosystem NEP based on an improved CASA model," *IEEE J. Sel. Topics Appl. Earth Observ. Remote Sens.*, vol. 16, pp. 1244–1255, 2023, doi: 10.1109/JSTARS.2022.3233128.

[12] A. Lin, H. Wu, W. Luo, K. Fan, and H. Liu, "How does urban heat island differ across urban functional zones? Insights from 2D/3D urban morphology using geospatial big data," *Urban Climate*, vol. 53, Jan. 2024, Art. no. 101787, doi: 10.1016/j.uclim.2023.101787.

[13] W. Yuan et al., "Increased atmospheric vapor pressure deficit reduces global vegetation growth," *Sci. Adv.*, vol. 5, 2009, Art. no. eaax1396, doi: 10.1126/sciadv.aax1396.

[14] B. O. Ogutu, J. Dash, and T. P. Dawson, "Developing a diagnostic model for estimating terrestrial vegetation gross primary productivity using the photosynthetic quantum yield and Earth observation data," *Glob. Change Biol.*, vol. 19, pp. 2878–2892, 2013, doi: 10.1111/gcb.12261.

[15] S. W. Running, R. R. Nemani, F. A. Heinsch, M. Zhao, M. Reeves, and H. Hashimoto, "A continuous satellite-derived measure of global terrestrial primary production," *BioScience*, vol. 54, pp. 547–560, 2004, doi: 10.1641/0006-3568(2004)054.

[16] J. L. Kalfas, X. Xiao, D. X. Vanegas, S. B. Verma, and A. E. Suyker, "Modeling gross primary production of irrigated and rain-fed maize using MODIS imagery and CO2 flux tower data," *Agricultural Meteorol.*, vol. 151, pp. 1514–1528, 2011, doi: 10.1016/j.agrformet.2011.06.007.

[17] S. Wang et al., "Improving the light use efficiency model for simulating terrestrial vegetation gross primary production by the inclusion of diffuse radiation across ecosystems in China," *Ecol. Complex*, vol. 23, pp. 1–13, 2015, doi: 10.1016/j.ecocom.2015.04.004.

[18] H. Yan et al., "Improved global simulations of gross primary product based on a new definition of water stress factor and a separate treatment of C3 and C4 plants," *Ecol. Model*, vol. 297, pp. 42–59, 2015, doi: 10.1016/j.ecolmodel.2014.11.002.

[19] W. Yuan et al., "Deriving a light use efficiency model from eddy covariance flux data for predicting daily gross primary production across biomes," *Agricultural Meteorol.*, vol. 143, pp. 189–207, 2007, doi: 10.1016/j.agrformet.2006.12.001.

[20] C. S. Potter et al., "Terrestrial ecosystem production: A process model based on global satellite and surface data," *Glob. Biogeochemical Cycles*, vol. 7, pp. 811–841, 1993, doi: 10.1029/93GB02725.

[21] Y. Zheng et al., "Improved estimate of global gross primary production for reproducing its long-term variation, 1982–2017," *Earth Syst. Sci. Data*, vol. 12, no. 4, pp. 2725–2746, Nov. 2020, doi: 10.5194/essd-12-2725-2020.

[22] L. -X. Zhang, D. -C. Zhou, J. -W. Fan, and Z. -M. Hu, "Comparison of four light use efficiency models for estimating terrestrial gross primary production," *Ecol. Model*, vol. 300, pp. 30–39, 2015, doi: 10.1016/j.ecolmodel.2015.01.001.

[23] S. Jiang et al., "Comparison of satellite-based models for estimating gross primary productivity in agroecosystems," *Agricultural Meteorol.*, vol. 297, 2021, Art. no. 108253, doi: 10.1016/j.agrformet.2020.108253.

[24] R. Yu, "An improved estimation of net primary productivity of grassland in the Qinghai-Tibet region using light use efficiency with vegetation photosynthesis model," *Ecol. Model*, vol. 431, 2020, Art. no. 109121, doi: 10.1016/j.ecolmodel.2020.109121.

[25] M. S. Biudes et al., "Gross primary productivity of Brazilian Savanna (Cerrado) estimated by different remote sensing-based models," *Agricultural Meteorol.*, vol. 307, 2021, Art. no. 108456, doi: 10.1016/j.agrformet.2021.108456.

[26] M. He et al., "Development of a two-leaf light use efficiency model for improving the calculation of terrestrial gross primary productivity," *Agricultural Forest Meteorol.*, vol. 173, pp. 28–39, May 2013, doi: 10.1016/j.agrformet.2013.01.003.

[27] X. Guan, J. M. Chen, H. Shen, and X. Xie, "A modified two-leaf light use efficiency model for improving the simulation of GPP using a radiation scalar," *Agricultural Forest Meteorol.*, vol. 307, Sep. 2021, Art. no. 108546, doi: 10.1016/j.agrformet.2021.108546.

[28] J. L. Monteith, "Solar radiation and productivity in tropical ecosystems," *J. Appl. Ecol.*, vol. 9, pp. 747–766, 1972, doi: 10.2307/2401901.

[29] J. L. Monteith, C. J. Moss, G. W. Cooke, N. W. Pirie, and G. D. H. Bell, "Climate and the efficiency of crop production in Britain. Philos," *Philos. Trans. Roy. Soc. B*, vol. 281, pp. 277–294, 1977, doi: 10.1098/rstb.1977.0140.

[30] S. Bao et al., "Environment-sensitivity functions for gross primary productivity in light use efficiency models," *Agricultural Meteorol.*, vol. 312, 2022, Art. no. 108708, doi: 10.1016/j.agrformet.2021.108708.

[31] D. Yang, X. Xu, F. Xiao, C. Xu, W. Luo, and L. Tao, "Improving modeling of ecosystem gross primary productivity through re-optimizing temperature restrictions on photosynthesis," *Sci. Total Environ.*, vol. 788, 2021, Art. no. 147805, doi: 10.1016/j.scitotenv.2021.147805.

[32] X. Yang et al., "Impacts of diffuse radiation fraction on light use efficiency and gross primary production of winter wheat in the North China Plain," *Agricultural Meteorol.*, vol. 275, pp. 233–242, 2019, doi: 10.1016/j.agrformet.2019.05.028.

[33] A. A. Ali et al., "Global-scale environmental control of plant photosynthetic capacity," *Ecological Appl., Publication Ecological Soc. Amer.*, vol. 25, pp. 2349–2365, 2015, doi: 10.1890/14-2111.1.

[34] J. Wu et al., "Partitioning controls on Amazon Forest photosynthesis between environmental and biotic factors at hourly to interannual timescales," *Glob. Change Biol.*, vol. 23, pp. 1240–1257, 2016, doi: 10.1111/gcb.13509.

[35] Z. Wu et al., "Climate data induced uncertainty in model based estimations of terrestrial primary productivity," *Environ. Res. Lett.*, vol. 12, 2017, Art. no. 064013, doi: 10.1088/1748-9326/aa6fd8.

[36] Y. Zhang et al., "A global moderate resolution dataset of gross primary production of vegetation for 2000–2016," *Sci. Data*, vol. 4, 2017, Art. no. 170165, doi: 10.1038/sdata.2017.165.

[37] T. Nakaji, R. Ide, H. Oguma, N. Saigusa, and Y. Fujinuma, "Utility of spectral vegetation index for estimation of gross CO2 flux under varied sky conditions," *Remote Sens. Environ.*, vol. 109, pp. 274–284, 2007, doi: 10.1016/j.rse.2007.01.006.

[38] F. Baret and G. Guyot, "Potentials and limits of vegetation indices for LAI and APAR assessment," *Remote Sens. Environ.*, vol. 35, pp. 161–173, 1991, doi: 10.1016/0034-4257(91)90009-U.

[39] F. Yang et al., "Hyperspectral estimation of corn fraction of photosynthetically active radiation," *Agricultural Sci. China*, vol. 6, pp. 1173–1181, 2007, doi: 10.1016/S1671-2927(07)60161-8.

[40] J. Liu, J. R. Miller, D. Haboudane, E. Pattey, and K. Hochheim, "Crop fraction estimation from casi hyperspectral data using linear spectral unmixing and vegetation indices," *Can. J. Remote Sens.*, vol. 34, pp. 124–138, 2008, doi: 10.5589/m07-062.

[41] P. H. Schuepp, M. Y. Leclerc, J. I. MacPherson, and R. L. Desjardins, "Footprint prediction of scalar fluxes from analytical solutions of the diffusion equation," *Boundary-Layer Meteorol.*, vol. 50, pp. 355–373, 1990, doi: 10.1007/BF00120530.

[42] L. Liang et al., "Remote sensing estimation and spatiotemporal pattern analysis of terrestrial net ecosystem productivity in China," *Remote Sens.*, vol. 14, no. 8, Jan. 2022, Art. no. 8, doi: 10.3390/rs14081902.

[43] H. Yan, Y. Fu, X. Xiao, H. Q. Huang, H. He, and L. Ediger, "Modeling gross primary productivity for winter wheat–maize double cropping system using MODIS time series and CO2 eddy flux tower data," *Agriculture, Ecosystems Environ.*, vol. 129, pp. 391–400, 2009, doi: 10.1016/j.agee.2008.10.017.

[44] A. A. Gitelson et al., "Relationship between gross primary production and chlorophyll content in crops: Implications for the synoptic monitoring of vegetation productivity," *J. Geophysical Res.*, vol. 111, 2006, Art. no. D08S11, doi: 10.1029/2005JD006017.

[45] H. Wu et al., "SALT: A multifeature ensemble learning framework for mapping urban functional zones from VGI data and VHR images," *Comput. Environ. Urban Syst.*, vol. 100, Mar. 2023, Art. no. 101921, doi: 10.1016/j.compenvurbsys.2022.101921.

[46] K. Fan, A. Lin, H. Wu, and Z. Xu, "Pano2Geo: An efficient and robust building height estimation model using street-view panoramas," *ISPRS J. Photogrammetry Remote Sens.*, vol. 215, pp. 177–191, Sep. 2024, doi: 10.1016/j.isprsjprs.2024.07.005.

[47] A. Lin, B. Huang, H. Wu, and W. Luo, "An MIU-based deep embedded clustering model for urban functional zoning from remote sensing images and VGI data," *Int. J. Appl. Earth Observation Geoinformation*, vol. 128, Apr. 2024, Art. no. 103689, doi: 10.1016/j.jag.2024.103689.

[48] J. Epiphanio and A. R. Huete, "Dependence of NDVI and SAVI on sun/sensor geometry and its effect on fAPAR relationships in Alfalfa," *Remote Sens. Environ.*, vol. 51, pp. 351–360, 1995, doi: 10.1016/0034-4257(94)00110-9.

[49] J. -L. Roujean and F. -M. Breon, "Estimating PAR absorbed by vegetation from bidirectional reflectance measurements," *Remote Sens. Environ.*, vol. 51, pp. 375–384, 1995, doi: 10.1016/0034-4257(94)00114-3.

[50] M. N. Merzlyak and A. Gitelson, "Why and what for the leaves are yellow in autumn? On the interpretation of optical spectra of senescing leaves (acerplatanoides L," *J. Plant Physiol.*, vol. 145, pp. 315–320, 1995, doi: 10.1016/S0176-1617(11)81896-1.

[51] S. B. Verma et al., "Annual carbon dioxide exchange in irrigated and rainfed maize-based agroecosystems," *Agricultural Meteorol.*, vol. 131, pp. 77–96, 2005, doi: 10.1016/j.agrformet.2005.05.003.

[52] L. Liang, Q. Wang, S. Qiu, D. Geng, and S. Wang, "NEP estimation of terrestrial ecosystems in China using an improved CASA model and soil respiration model," *IEEE J. Sel. Topics Appl. Earth Observ. Remote Sens.*, vol. 16, pp. 10203–10215, 2023, doi: 10.1109/JSTARS.2023.3325774.
[53] K. Kanniah, J. Beringer, N. Tapper, L. Hutley, and X. Zhu, "Evaluation of collections 4 and 5 of the MODIS gross primary productivity product and algorithm improvement at a tropical Savanna site in Northern Australia," *Remote Sens. Environ.*, vol. 113, pp. 1808–1822, 2009, doi: 10.1016/j.rse.2009.04.013.
[54] Y. Peng and A. A. Gitelson, "Remote estimation of gross primary productivity in soybean and maize based on total crop chlorophyll content," *Remote Sens. Environ.*, vol. 117, pp. 440–448, 2012, doi: 10.1016/j.rse.2011.10.021.
[55] M. Jung et al., "Scaling carbon fluxes from eddy covariance sites to globe: Synthesis and evaluation of the FLUXCOM approach," *Biogeosciences*, vol. 17, pp. 1343–1365, 2020, doi: 10.5194/bg-17-1343-2020.
[56] K. Schaefer et al., "A model-data comparison of gross primary productivity: Results from the North American carbon program site synthesis," *J. Geophys Res. Biogeosciences*, vol. 117, 2012, Art. no. 03010, doi: 10.1029/2012JG001960.
[57] Y. Sun, D. Peng, X. Guan, D. Chu, Y. Ma, and H. Shen, "Impacts of the data quality of remote sensing vegetation index on gross primary productivity estimation," *GISci. Remote Sens.*, vol. 60, no. 1, Dec. 2023, Art. no. 26201, doi: 10.1080/15481603.2023.2275421.
[58] M. Aubinet, T. Vesala, and D. Papale, *Eddy Covariance: A Practical Guide to Measurement and Data Analysis*. Berlin, Germany: Springer Science & Business Media, 2012.
[59] X. Tian, F. Minunno, T. Cao, M. Peltoniemi, T. Kalliokoski, and A. Mäkelä, "Extending the range of applicability of the semi-empirical ecosystem flux model PRELES for varying forest types and climate," *Glob. Change Biol.*, vol. 26, pp. 2923–2943, 2019, doi: 10.1111/gcb.14992.
[60] J. Bremer and S. Karsten, "Identification of a general light use efficiency model for gross primary production," *Biogeosciences*, vol. 8, pp. 999–1021, 2011, doi: 10.5194/bg-8-999-2011.
[61] I. McCallum et al., "Improved light and temperature responses for light-use-efficiency-based GPP models," *Biogeosciences*, vol. 10, pp. 6577–6590, 2013, doi: 10.5194/bg-10-6577-2013.
[62] Z. Zhang, L. Zhao, and A. Lin, "Evaluating the performance of sentinel-3A OLCI land products for gross primary productivity estimation using AmeriFlux data," *Remote Sens.*, vol. 12, no. 12, Jan. 2020, Art. no. 12, doi: 10.3390/rs12121927.
[63] N. Zhang and C. Liu, "Simulated water fluxes during the growing season in semiarid grassland ecosystems under severe drought conditions," *J. Hydrol.*, vol. 512, pp. 69–86, 2014, doi: 10.1016/j.jhydrol.2014.02.056.
[64] W. Cai et al., "Large differences in terrestrial vegetation production derived from satellite-based light use efficiency models," *Remote Sens.*, vol. 6, pp. 8945–8965, 2014, doi: 10.3390/rs6098945.

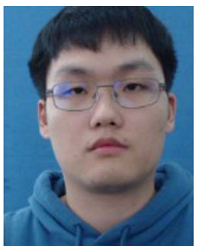

Zeyang Wei received the M.Sc. degree in agricultural engineering and information technology, in 2023, from Hubei University, Wuhan, China, where he is currently working toward the Ph.D. degree in ecology.

His research interests include ecological remote sensing and quantitative remote sensing.

Hai Xiao received the bachelor's degree in land resource management.

He is the Deputy Director of the Second Institute of Surveying and Mapping of Hunan Province, China. He is responsible for production management and fieldwork-related safety supervision. His duties also include overseeing basic geographic surveys and monitoring, thematic investigations, urban spatial monitoring, carbon sink monitoring, and analysis and evaluation of survey and monitoring results. His professional interests include geospatial data production, environmental monitoring, and applications of remote sensing technologies in urban and ecological assessment.

Lu Zhang received the B.Sc. degree in geographic information science and the M.Sc. degree in agricultural engineering and information technology from Hubei University, Wuhan, China, in 2020 and 2023, respectively.

Her research interest focuses on ecological remote sensing.

Lifei Wei received the Ph.D. degree in photogrammetry and remote sensing from the State Key Laboratory of Information Engineering in Surveying, Mapping and Remote Sensing, Wuhan University, Wuhan, China, in 2018.

Since 2014, he has been a Professor and Ph.D. Supervisor with the School of Resources and Environmental Science, Hubei University, Wuhan, China.. His research interests include intelligent processing of remote sensing imagery, ecological and agricultural remote sensing, and geospatial Big Data analysis and visualization.

Qikai Lu received the B.S. degree in remote sensing from the School of Remote Sensing and Information Engineering, Wuhan University, Wuhan, China, in 2011, and the Ph.D. degree in photogrammetry and remote sensing from the State Key Laboratory of Information Engineering in Surveying, Mapping and Remote Sensing, Wuhan University, in 2016.

Since 2019, he has been with the School of Resources and Environmental Science, Hubei University, Wuhan, China.

His research interests include remote sensing image processing, urban remote sensing, and machine learning.